Monitoring of engine oil aging by diffusion and low-field nuclear magnetic resonance relaxation

E. Förster [a], C.C. Fraenza [b], J. Küstner [a], E. Anoardo [b], H. Nirschl [a], G. Guthausen [a,c,*]

[a] Institute of Mechanical Process Engineering and Mechanics, Karlsruhe Institute of Technology, Karlsruhe, Germany
[b] Facultad de Matemática, Astronomía, Física y Computación, Universidad Nacional de Córdoba and IFEG – CONICET, Ciudad Universitaria X5000HUA, Córdoba, Argentina
[c] Engler-Bunte-Institute, Water Chemistry and Water Technology, Karlsruhe Institute of Technology, Karlsruhe, Germany

A B S T R A C T

Time domain, also named lowfield nuclear magnetic resonance is used to monitor oil degradation by measuring relaxation and diffusion. As quality control of oils is indispensable to optimize oil change intervals while simultaneously preventing machinery damage, the technique was applied to detect the degradation state of engine oils as time domain nuclear magnetic resonance is known as a well suited tool to measure quality control parameters for example in food industry. Correlations with commonly applied oil analytics like viscosity measurements and inductively coupled plasma optical emission spec trometry allow to interpret relaxation and diffusion data in detail and finally to deepen the understanding of oil aging processes. Additionally, the measurement temperature was varied to achieve the maximum sensitivity towards oil aging. Low field NMR is not only realized in form of table top instruments, but also in form of field cycling and single sided NMR devices. Fast field cycling as well as single sided NMR were also explored to study oil aging and to provide valuable insight. The latter device was used to obtain information about translational diffusion and transverse relaxation of oils simultaneously.

Keywords:
Engine oil degradation
NMR relaxometry
NMR diffusometry
Lubricant oils
Oil condition monitoring

1. Introduction

Oils are an integral part of an engine and have a significant influence on its functional and damage behavior. During engine operation, the physico chemical properties and accordingly the performance of the oils change with the environmental stress. Changes predominantly occur due to particulate contamination, oxidation, mechanical and thermal stress [1,2].

Engine oils mostly consist of a base oil and 5 20% of additives [3]. The characteristic properties of lubricant oils are determined by the additives and depend on the application. A deep under standing of functionality and aging processes is indispensable also because of the diversity of nowadays existing oils. Many com monly accepted methods for oil analysis exist like infrared (IR) spectroscopy, mass spectrometry coupled with gas chromatogra phy (GC MS), inductively coupled plasma optical emission spectrometry (ICP OES) and nuclear magnetic resonance (NMR) spectroscopy. Previous studies proved high field NMR spectroscopy to be a good method for the analysis of chemical composition of oils [4 8]. Besides the degradation of additives also the formation of oxidation products is detected. In conventional ^{1}H one dimensional spectroscopy, the peak overlap complicates the detailed interpretation of these 1D spectra.

An alternative to characterize motor oils came into the focus of research and bases on the investigation of molecular dynamics using low field NMR (LF NMR) relaxation and diffusion, often called time domain NMR (TD NMR) combined with adequate data modeling [5,9 11]. Also with the perspective of quality control (QC) this approach is promising. These devices in contrast to highfield NMR are much cheaper and robust regarding environ mental influences. Especially in food industry TD NMR has become an important tool for QC e.g. to analyze moisture and water content in the presence of lipids [12 14] or to determine the solid fat content in fat mixtures to name two prominent examples [15 17].

This study targets the monitoring of engine oil degradation in a motor test rig using NMR relaxation and diffusion. Correlations between established analysis methods like viscosity measurement and ICP OES and the NMR parameters are explored with respect to the suitability as a tool for QC on oil degradation. In order to find the maximum sensitivity regarding oil aging, diffusion and relax ation were measured at different temperatures. As both, relaxation and diffusion, show sensitivities towards oil aging which strongly depend on the oil's composition and aging processes, a grouping

* Corresponding author at: EBI and MVM at KIT, Adenauerring 20b, D-76131 Karlsruhe, Germany.
E-mail address: gisela.guthausen@kit.edu (G. Guthausen).

of the measurement methods was attempted by exploiting single sided NMR, too. It is well known that transverse relaxation and diffusion determine the signal decay in multi echo sequences due to the large static magnetic field gradients of these devices. These measurements are complementary to the named ones and open up the field to construct dedicated sensors for QC of engine oils.

2. Theory

In order to obtain characteristic NMR parameters to describe the state of engine oils, data modeling is a common approach, which essentially results in a reduction of the dimensionality of the data sets. As oils are multi component systems, the question arises how to model relaxation and diffusion decays adequately. Commonly applied methods are modeling via exponentially decay ing functions, the numerical approach of inverse Laplace transform as well as the consideration of discrete distributions of relaxation rates and diffusion coefficients.

In ^{1}H NMR, most often the homonuclear dipolar couplings dom inate longitudinal as well as transverse relaxation. However, para magnetic relaxation enhancement (PRE) cannot be neglected if magnetic moieties are present in a sample. Especially the trans verse relaxation is enhanced considerably by (super) paramag netic particles, whereas the longitudinal relaxation is more sensitive to small paramagnetic ions, molecules or clusters with longer correlation times of the unpaired electronic states [18 21].

2.1. Γ distribution for describing relaxation and diffusion data

The main advantage of an analytical model considering explic itly a distribution is its numerical stability when compared with numerical inversion algorithms as inverse Laplace transform for example. In the case of the Γ distribution mean values of relax ation rate or diffusion coefficient and the corresponding distribu tion width are obtained directly. The echo decay for diffusion can be written within this model as [22]:

$$I(t) \quad I_0\left(1+\frac{t\sigma_G^2}{\langle D\rangle}\right)^{\frac{\langle D\rangle^2}{\sigma_G^2}} \tag{1}$$

where I_0 is the signal intensity corresponding to the condition $k \quad (\gamma g\delta)^2(\Delta \quad \frac{\delta}{3}) \quad 0$, γ being the gyromagnetic ratio, g the gradient amplitude, δ the gradient pulse duration and Δ the diffusion time. In Eq. (1) $\langle D\rangle$ corresponds to the mean value of the self diffusion coef ficient and σ_G to the width of the Gamma distribution P_G (indicated by "G"). P_G as a normalized distribution density has the inverse unit of the described parameter, i.e. s/m^2 in the case of diffusion and s in the case of relaxation distribution. Please note that the approach is not limited to a single distribution, but can be extended to multi modality. Similarly, in the case of transverse relaxation the magne tization decay can be expressed as [5]:

$$M(t) \quad M_0\left(1+\frac{t\sigma_{R2}^2}{\langle R_2\rangle}\right)^{\frac{\langle R_2\rangle^2}{\sigma_{R_2}^2}} \tag{2}$$

with the initial magnetization M_0, the mean transverse relaxation rate $\langle R_2\rangle$, and the distribution width σ_{R2}. The magnetization M depends on the time t of the NMR experiment.

Also the mean longitudinal relaxation rate $\langle R_1\rangle$ and the distribu tion width σ_{R1} can be obtained within the Γ model with $n \quad 0$ for saturation recovery and $n \quad 1$ for inversion recovery when model ing the magnetization according to Eq. (3):

$$M(t) \quad M_0\left(1 \quad 2^n\left(1+\left(\frac{t\sigma_{R1}^2}{\langle R_1\rangle}\right)\right)^{\frac{\langle R1\rangle^2}{\sigma_{R1}^2}}\right) \tag{3}$$

2.2. Dispersion of spin lattice relaxation

The spin lattice relaxation (R_1) shows a pronounced dispersion as a function of Larmor frequency. It is sensitive to the dynamic states of a molecular system, thus being a powerful tool for the characterization of a variety of materials [23]. Measurements can be conveniently performed by fast field cycling (FFC) NMR relax ometry [23 25]. It was already used to study different motor oils and their aging [20]. There are two main questions arising within this context: (i) at which Larmor frequency the maximum sensitiv ity to oil aging is expected (as observed by a change in spin lattice relaxation) and (ii) is the dispersion of the spin lattice relaxation sensitive to oil aging? Both aspects, as revealed by the measured dispersion curves, can be conveniently quantified in terms of the involved physico chemical parameters. In order to obtain the set of parameters that characterize the sample, a model that consis tently explains the observed dispersions is needed.

Apart from a possible PRE caused by abrasion, leading to (super) paramagnetic particles in the aged oils, ^{1}H spin lattice relaxation is dominated by homonuclear dipolar relaxation. As a first approach, the ^{1}H spin lattice relaxation dispersion can be modeled by considering translational diffusion plus a Lorentzian term for the account of molecular rotations (or functional groups of them) [26].

2.2.1. Contribution of translational diffusion to R_1

The translational diffusion of molecules statistically affects the homonuclear dipolar interaction (also named dipol dipol interac tion, therefore abbreviated as DD) on short time scales and there fore leads to spin lattice relaxation [27,28]. To describe the spin lattice relaxation due to translational diffusion $R_{1,DD}^{Tr}$ under the assumption of random motion and small diffusion correlation times τ_D the following expression was found [24,26]:

$$R_{1,DD}^{Tr} \quad \frac{A_D\tau_D}{x^4}\left[j(x)+j\left(\sqrt{2x}\right)\right], \tag{4}$$

where A_D is a constant related to the dipolar couplings squared, and $j(x)$ is the spectral density given by:

$$j(x) \quad \frac{x}{2} \quad \frac{1}{x}+\frac{x}{2}e^{\ x}\left[\left(1 \quad \frac{2}{x^2}\right)\sin(x)+\left(1+\frac{4}{x}+\frac{2}{x^2}\right)\cos(x)\right] \tag{5}$$

In Eqs. (4) and (5), $x \quad (\omega_L\tau_D/2)^{1/2}$ with the diffusion correlation time τ_D and $\omega_L \quad 2\pi\upsilon_L$, where υ_L is the Larmor frequency.

2.2.2. Contribution of rotations and vibrations to R_1

Both molecular motions are usually effective in relaxing nuclear magnetization. In an extremely simplified picture, we may con sider an average correlation time. Dominant Lorentzian processes with correlation times in the range of 10^{-8} 10^{-9} s are usually ascribed to rotations of molecules [26,29]. Fast motions and reori entations of functional groups are usually non dispersive and char acterized by shorter correlation times. The spin lattice relaxation rate due to rotational motions $R_{1,DD}^{Rot}$ can be described as:

$$R_{1,DD}^{Rot} \quad A_R\left[\frac{\tau_R}{1+(\omega_L\tau_R)^2}+\frac{4\tau_R}{1+(2\omega_L\tau_R)^2}\right], \tag{6}$$

where τ_R is the rotational correlation time and A_R a constant again determined by the dipolar couplings squared.

Assuming the statistical independence of these two contribu tions, the total spin lattice relaxation rate due to homonuclear dipolar relaxation can be written as [24]:

$$R_{1,DD} \quad R_{1,DD}^{Tr}+R_{1,DD}^{Rot}. \tag{7}$$

3. Materials and methods

Nine engine oil samples of specific runtimes from an engine test rig were investigated. The total runtime of the engine t_{Engine} was 1452 h. Oil changes were performed after 665 h and 1251 h. The density δ_{oil} of the fresh oil is 845 kg/m^3. The kinematic viscosity ν was measured at 313 K (Table 1).

In order to get information about impurities in the oils, element analysis was performed using ICP OES. ICP OES results do not give information about the oxidation state and thus about the magnetism of the measured elements. As it is well known that PRE is rather strongly contributing to transverse and longitudinal relaxation, and as additionally (super) paramagnetic abrasion occurs in engines, a first approach was made: The amounts of iron, copper and molybdenum were summarized in a worst case scenario of maximum (super) paramagnetic concentration in Table 2. c_{para} then is the maximum total concentration of potentially paramagnetic compounds.

Longitudinal relaxation was measured via fast FFC NMR using the Stelar SPINMASTER FFC2000 NMR relaxometer and with a Bruker "the minispec" mq20 time domain NMR with a ^{1}H Larmor frequency of 20 MHz. R_1 dispersions obtained by FFC NMR were measured in a Larmor frequency range from 30 kHz to 15 MHz. Compensated pre polarized (PP) and non polarized (NP) sequences [25] were applied. The measurement temperature was varied between 283 K and 353 K and kept constant by active thermosetting the sample chamber in the corresponding NMR probes. R_1 relaxation measurements at 20 MHz using the Bruker "the minispec" mq20 analyzer were performed by progressive saturation recovery (Table 3). The measurement temperature for these measurements was varied between 293 K and 373 K.

Transverse relaxation was measured by the 20 MHz time domain Bruker "the minispec" mq20 applying a CPMG (Carr Purcell Meiboom Gill) multiecho sequence [30] (Table 3). As in most of the LF TD NMR instruments no chemical shift resolution is available, the echo maxima were processed for determination of magnetization decay. Care was taken to not loose fast decaying magnetization components via variation of the echo time, resulting in the final value of 250 μs (Table 3). For modeling the magnetization decays, the Γ distribution approach was applied (Eq. (2)) [5].

Diffusion measurements were performed on a 200 MHz instrument (DRX, Bruker) equipped with a Diff30 probe with gradients up to 12 T/m using a Pulsed Field Gradient Stimulated Echo sequence (PFG STE, for example [31]) (Table 4). Temperature was varied between 293 and 373 K. It is given for each measurement in the description of the figures.

The pseudo 2D data sets were 1D Fourier transformed along the dimension of data acquisition. The signal attenuation in the spectra was recorded as a function of q^2 $(\gamma\delta g)^2$. Data was analyzed using the Γ distribution model (Eq. (1)) [22]. To obtain a representative measure for a possible QC application of diffusion NMR, only the signal around 1.3 ppm in the aliphatic region was analyzed considering that the most prominent peak in oil spectra is the peak of the aliphatic CH_2 groups together with the nearby CH_3 groups which mainly belong to the oil molecules, therefore exhibiting the same diffusion coefficient. As the concentration of oils is much larger than that of additives, no differentiation was made along the gradient axis. The gradient was stepped within the significant range providing the complete range of signal attenuation. Care was taken to avoid artefacts at small gradient amplitudes.

To investigate the possibilities of TD NMR in QC of oil all samples were measured in their original state without any dilution. A single sided NMR device inspired by the NMR MOUSE® (Mobile Universal Surface Explorer), which has been developed at RWTH Aachen [32], was used. Major advantages of these devices are the small size, low costs, independence of sample geometry and therefore the minimum sample preparation. As the sample tube only has to be put onto the probe, the method is completely non destructive and non invasive with low costs for sample handling, preparation or dilution. Due to the high static magnetic field gradients of these devices, relaxation and diffusion can be measured simultaneously. Furthermore, there is no serious limitation in the case of (super) paramagnetic contaminants being present in aged oils. CPMG was used while varying the echo time $2\tau_E$, where $2\tau_E$ is the time between two refocusing pulses, with the inherent possibility to differentiate the effect of translational diffusion from transverse relaxation [33]. The magnetization decay directly depends on the experiment time t $n * 2\tau_E$ and can be described by:

$$M(t) \quad M_0 \exp\left(\quad t(R_2 + \frac{1}{12}\gamma^2 D g^2 (2\tau_E)^2) \right) \quad M_0 \exp(\quad tR_{2eff}) \qquad (8)$$

with the static, effective field gradient g of the main magnetic field B_0, the diffusion coefficient D and the effective transverse relaxation rate R_{2eff}. As the magnetization decay depends mono exponentially on the experiment time t when assuming a simple liquid, combined diffusion and transverse relaxation can be measured resulting in R_{2eff} [33 35]. The device used in this work has a Larmor frequency of 22.5 MHz, which corresponds to a magnetic field of 0.528 T. The echo time τ_E was varied between 0.15 ms and 0.95 ms in steps of 0.1 ms. For each echo time, 160 scans were acquired and averaged. In order to obtain R_{2eff} the data was analyzed using the Γ distribution model while allowing for a small offset in the data.

In the following, no error bars are shown. However, it should be noted at this point that the deviations of the measured data amount to a maximum of 10%.

Table 1
Characteristics of the investigated oil samples. The stars indicate the samples being used to calculate the relaxivities (see 4.1.3).

Oil sample	Oil change interval	Engine runtime t_{Engine} [h]	Oil runtime t_{Oil} [h]	Kinematic viscosity ν [mm^2/s] at 313 K
1*	1st interval	0	0	55.69
2		223	206	55.19
3		429	412	58.29
4		665	648	65.60
Oil change				
5*	2nd interval	845	180	56.51
6		1072	407	59.31
7		1251	591	64.68
Oil change				
8*	3rd interval	1365	109	56.58
9*		1452	196	57.17

Table 2
Potentially paramagnetic compounds of the oil samples listed in Table 1, measured by ICP-OES.

Oil sample	Oil change interval	Iron Fe [g(Fe)/kg(total)]	Molybdenum Mo [g(Mo)/kg(total)]	Copper Cu [g(Cu)/kg(total)]	c_{para} [g(c_{para})/kg(total)]
1*	1st interval	0.001	0.046	0.001	0.048
2		0.011	0.051	0.022	0.084
3		0.020	0.057	0.032	0.109
4		0.032	0.063	0.040	0.135
Oil change					
5*	2nd interval	0.008	0.053	0.011	0.072
6		0.014	0.058	0.015	0.087
7		0.019	0.061	0.017	0.097
Oil change					
8*	3rd interval	0.006	0.051	0.005	0.062
9*		0.016	0.055	0.010	0.081

Table 3
Experimental parameters for R_1 and R_2 relaxation measurements using a Bruker "the minispec" mq 20 and the FFC-relaxometer.

Measurement parameter	for R_1 TD-NMR (progressive saturation)	for R_2 TD-NMR (CPMG)	for FFC-NMR
90° pulse duration	5.52 μs	5.52 μs	7 μs
180° pulse duration	11.04 μs	11.04 μs	–
Echo time τ_E	–	250 μs	–
First recovery delay	3 ms	–	–
Increment factor	1.2	–	–
Last recovery delay	1 s (at 293 K)–3.7 s (at 373 K)	–	–
Polarization time	–	–	0.5 s
Polarization field	–	–	15 MHz
Detection field	–	–	14.19 MHz
Profile points	–	–	20
Number of points per field	32	1200 (at 293 K)–11,000 (at 373 K)	16 blocks
Recycle delay	0.06 s	1 s	0.3 s
Number of scans	16	16	4

Table 4
Experimental parameters for diffusion measurements.

Measurement parameter	Value
First delay	5 ms
Gradient pulse duration δ	5.5 ms (at 293 K, 303 K) and 3 ms (at 313 K)
Maximum gradient amplitude g	3–10 T/m
Diffusion time Δ	100 ms
Acquired data points	8192
Repetition time	1.5 s

4. Results and discussion

4.1. NMR relaxation

First, the dispersion of R_1, second the R_2 relaxation rates will be discussed and subsequently related to classic parameters like viscosity and paramagnetic impurities.

4.1.1. Dispersion of the longitudinal relaxation

R_1 values were determined by a mono exponential fit on the measured magnetization evolution. The application of the Γ fit was exemplarily checked and led, independent of the Larmor frequency, to 10% higher mean relaxation rates compared to the rates obtained by a mono exponential fit. The relaxation dispersion shows clear signatures of aging, exemplarily shown for the first oil change interval in Fig. 1a. With increasing runtime the relaxation rates increase. The differences in $R_1(\nu_0)$ between the oils additionally increase with decreasing Larmor frequency. Regarding R_1 as a function of the Larmor frequency ν_0 and the engine runtime t_{Engine} in Fig. 1b, also the oil changes can nicely be detected. Thus, the largest differences between the aged oils are found at 30 kHz leading to the conclusion that, when aiming for a sensitive analytical QC tool exploiting R_1, longitudinal relaxation has to be measured at very low magnetic fields. According to Eq. (7), the dipolar spin lattice relaxation dispersion of liquids is dominated by the two main relaxation mechanisms, the translational diffusion and the molecular motions. Applying these equations, the longitudinal relaxation dispersion (Fig. 1a) can be modeled with parameters summarized in Table 5 [26].

4.1.2. Transverse relaxation

In contrast to longitudinal relaxation, transverse relaxation is less dependent on the external magnetic field. R_2 was measured at 20 MHz using the Bruker "the minispec" mq20. The Γ distribution model seemed to describe oil transverse relaxation data in the physically most meaningful way [5]. Therefore, the relaxation data has been processed using this model. With increasing engine runtime the magnetization decays faster, exemplarily shown for the first oil change interval depicted in Fig. 2a. The corresponding relaxation distributions (Fig. 2b) analyzed by the Γ distribution model show an increase in the mean relaxation rate as well as in the distribution width with increasing engine runtime t_{Engine}.

Changes in the distribution widths over the runtime are a first sign for changes of the oils' composition. Also oil changes can nicely be detected as jumps in the mean transverse relaxation rate $\langle R_2 \rangle$ after an oil change. $\langle R_2 \rangle$ starts to increase again with engine time (Fig. 3).

4.1.3. Relation to viscosity and paramagnetic impurities

In order to correlate these findings to common analytical measures in the field of oil QC, viscosity data as well as particulate impurities were considered (Table 1). Both parameters increase with increasing oil runtime t_{Oil}. According to relaxation theory, the most prominent ^{1}H relaxation path in diamagnetic liquids is

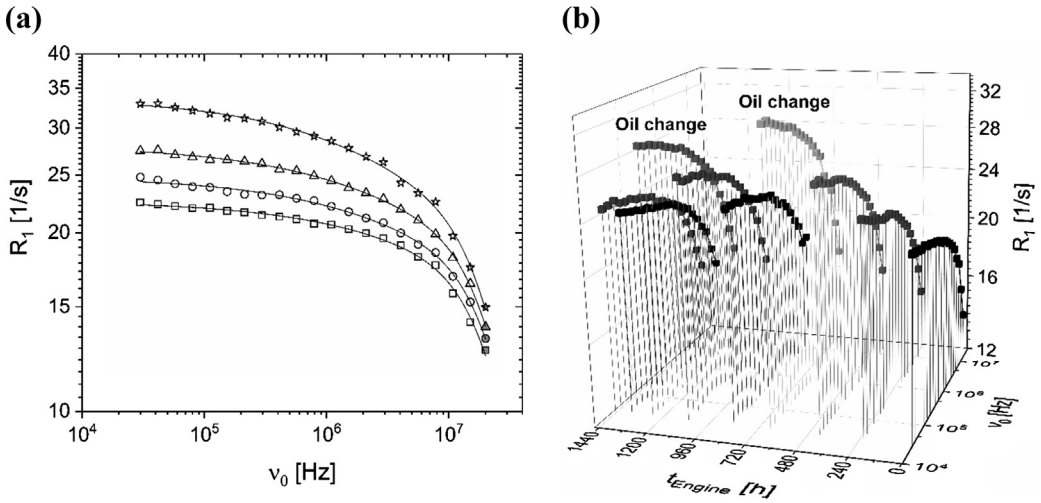

Fig. 1. Relaxation dispersion of longitudinal relaxation rate between 30 kHz and 15 MHz measured by the FFC2000 NMR relaxometer. All data was measured at 298 K. (a) Relaxation dispersion of longitudinal relaxation rate measured on fresh (□) and three used oils – t_{Engine}= 223 h (○), 429 h (△) and 665 h (☆) of the first interval. The points at 20 MHz (gray) were measured using the Bruker "the minispec" mq20. The black lines show the fit according to Eq. (7). (b) R_1 as a function of the engine runtime t_{Engine} and the Larmor frequency ν_0. R_1 increases with increasing runtime, the biggest differences being at 30 kHz. Oil changes can be detected.

Table 5
Parameters of the fits of Eq. (7) to the data in Fig. 1a (black lines).

Parameters	Engine runtime t_{Engine}			
	0 h	223 h	429 h	665 h
$\sqrt{A_D}$(kHz)	12 ± 11	11 ± 8	11 ± 6	13 ± 8
$\tau_D(10^{-7}$ s)	1.27 ± 0.76	1.74 ± 0.74	2.03 ± 0.45	2.12 ± 0.63
$\sqrt{A_R}$(kHz)	34 ± 6	35 ± 5	36 ± 4	36 ± 5
$\tau_R(10^{-9}$ s)	2.91 ± 0.17	2.84 ± 0.18	3.04 ± 0.11	3.22 ± 0.20

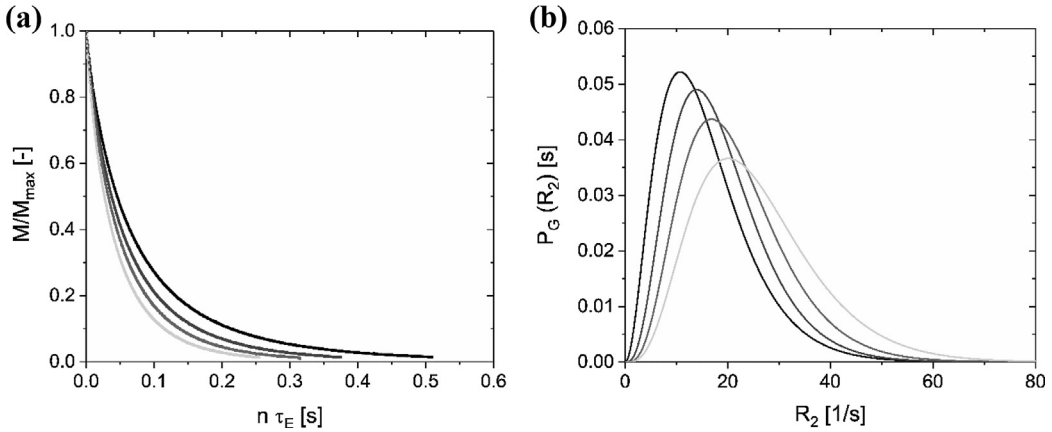

Fig. 2. (a) Transverse magnetization decays for oils of the first oil change interval measured at 298 K: 0 h (black), 226 h (dark gray), 429 h (middle gray), 665 h (light gray). With increasing runtime, the transverse magnetization decays faster. (b) The relaxation rate distribution P_G depends on the engine runtime t_{Engine}, also shown for the first oil change interval – 0 h (black), 226 h (dark gray), 429 h (middle gray), 665 h (light gray). With increasing engine runtime, an increase in the distribution width as well in as the mean relaxation rate is observed.

due to fluctuations in the homonuclear dipolar couplings [27]. Paramagnetic substances lead to the additional non negligible relaxation PRE. Thus, for oils containing paramagnetic particulate contaminations, besides fluctuations of the ^{1}H ^{1}H dipolar interac tion, those of the hyperfine interactions leading to PRE also have to be taken into account.

In a first crude approximation, the paramagnetic relaxation enhancement is related to the proportion of paramagnetic particu late contaminants in the oil, and the dipolar interaction can be related to viscosity. When measuring the relaxation rate and knowing the viscosity as well as the concentration of paramagnetic contaminants c_{para}, the contribution of dipolar interaction and PRE can be separated when first quantifying the PRE and second using the analoguos equation to Eq. (7) for dipolar relaxation and PRE. The relaxation rate due to PRE $R_{i,PRE}$ is known to be proportional to the particles concentration and to their relaxivity r_i:

$$R_{i,PRE} \quad r_i c_{para} \tag{9}$$

The mean relaxation rate now can be calculated in a first approach by:

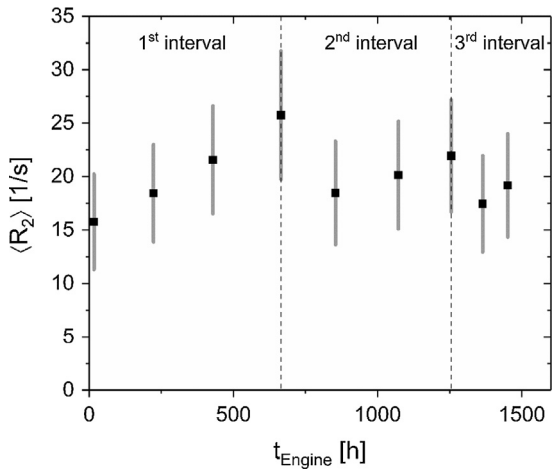

Fig. 3. The mean transverse relaxation rate $\langle R_2 \rangle$ and its distribution width (represented in form of error bars) depend on the engine runtime t_{Engine}, measured at 298 K. With increasing runtime t_{Oil}, the mean relaxation rate increases. Oil changes can be detected as $\langle R_2 \rangle$ drastically decreases after an oil change and then starts to increase again.

$$R_{i,mean} \quad R_{i,PRE} + R_{i,DD} \tag{10}$$

Due to the fact that four of the analysed oils show similar values of viscosity v but different relaxation rates R_1, $\langle R_2 \rangle$ and c_{para} at the same temperature of 313 K (Tables 1 and 2 marked with *), these samples were well suited as a basis for an estimate of r_1 and r_2. In a linear fit of R_1 and respectively of $\langle R_2 \rangle$ versus c_{para} (Eq. (9)), the corresponding relaxivity are given by the slope. The longitudinal relaxivity has a value of $r_1 \quad 51.22 \frac{kg(total)}{g(c_{para})s}$, the transverse relaxivity of $r_2 \quad 93.96 \frac{kg(total)}{g(c_{para})s}$, when assuming that the oxidation states of Fe, Cu and Mo detected by ICP OES are completely paramagnetic. This assumption is a worst case estimation, as not all of the amounts measured via ICP OES are necessarily paramagnetic. Under this assumption the contribution of homonuclear dipolar relaxation can be determined according to Eq. (10). It can nicely be seen that the dipolar relaxation for both, longitudinal and transverse relaxation, stays almost constant (Fig. 4). Analyzing the PRE relaxation rate as a function of the oil runtime t_{Oil}, the contamination is slightly higher in the first interval than in the following ones. As the motor was completely new at $t_{Engine} \quad 0$ h, and abrasion phenomena especially take place during the first operating hours the highest amount of particulate contamination occurs in the first interval. As expected for particulate paramagnetic impurities, the PRE contribution has a larger influence on the total transverse relaxation rate than on the total longitudinal relaxation rate.

4.2. Diffusion

Diffusion measurements were performed at different temperatures and were analyzed within the Γ distribution model (Eq. (1)) [22].

With increasing oil runtime t_{oil} the mean diffusion coefficient $\langle D \rangle$ clearly decreases (Fig. 5b). After 665 h and 1251 h, oil changes were performed. As a consequence of adding fresh oil, $\langle D \rangle$ directly increases drastically and then starts to decrease again. The same behavior was observed for the third interval. The diffusion coefficient distribution broadens slightly with increasing t_{Oil} whereas the distribution width of the oil sample after t_{Engine} 665 h again is slightly smaller (Fig. 5a). Changes in the oil composition are the reason for this change. 1D ^{1}H spectra (not shown) e.g. revealed changes in the aromatic spectral region, as polycyclic aromatic hydrocarbons (PAH) are formed due to incomplete combustion. Also the depletion of additives was detected [4,5]. Compared to transverse and longitudinal relaxation at low magnetic fields, $\langle D \rangle$ (measured at 200 MHz) is less sensitive towards oil aging in this special case of engine oils. Furthermore, the opposite trend compared to $\langle R_2 \rangle$ is observed, as $\langle D \rangle$ decreases and $\langle R_2 \rangle$ increases with increasing oil runtime.

Evaporation of volatile oil compounds and formation of oil insoluble compounds might be the reason for the decrease in $\langle D \rangle$ [8]. The diffusion coefficient is given by the squared mean displacement in a certain time period in the picture of thermal Brownian motion and is directly related to viscosity. Many relations exist [36]. A simple and simultaneously most common representation is provided by the Stokes Einstein relation [37]:

$$D \quad \frac{k_B T}{6\pi v \delta_{oil} R} \tag{11}$$

with the Boltzmann constant k_B, the absolute temperature T, the kinematic viscosity v and the density δ_{oil} of the media. R is the radius of diffusing moieties.

Plotting $\langle D \rangle$ over the inverse kinematic viscosity leads to the expected increase in $\langle D \rangle$ with inverse viscosity v (Fig. 6). Applying

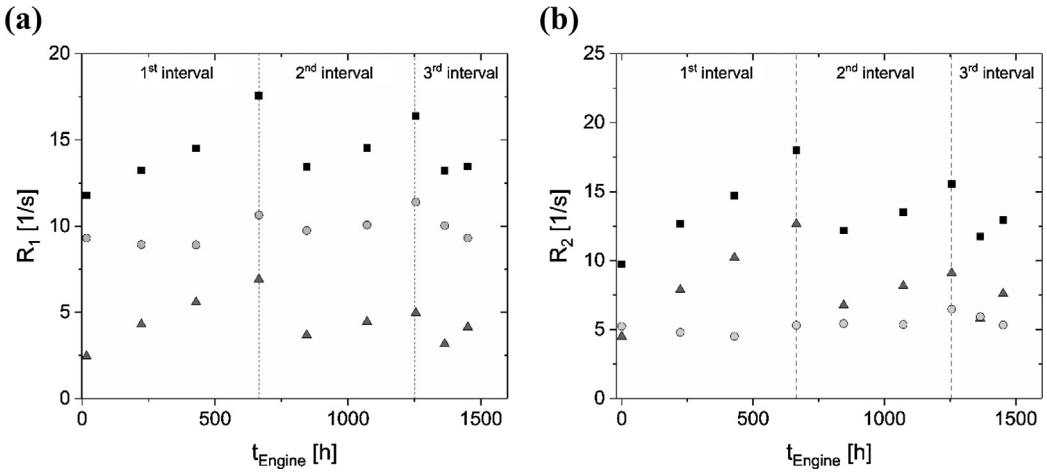

Fig. 4. (a) Longitudinal relaxation rate and (b) transverse relaxation rate (black □) and the contributions of dipolar (light gray ○) and paramagnetic relaxation (dark gray △) as a function of the engine runtime t_{Engine}. R_1 and $\langle R_2 \rangle$ were measured at 313 K as was the viscosity. Dashed lines indicate the oil changes.

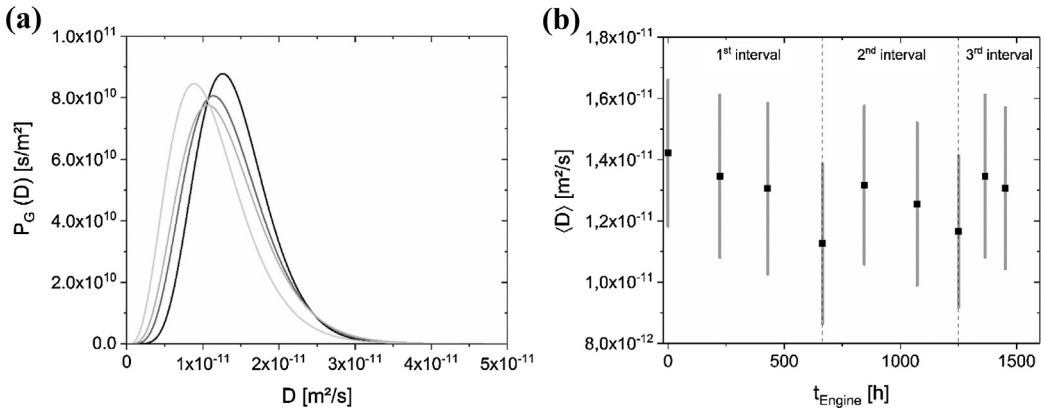

Fig 5. (a) Distribution P_G of the diffusion coefficient D for different engine runtimes t_{Engine} in the first oil change interval measured at $T = 293$ K – 0 h (black), 226 h (dark gray), 429 h (middle gray), 665 h (light gray). With increasing t_{Engine} a decrease in the distribution width was observed. The mean diffusion coefficient decreases with t_{Engine}. (b) Mean diffusion coefficient $\langle D \rangle$ and distribution widths (presented in form of error bars) as a function of the engine runtime t_{Engine}, measured at 293 K. Dashed lines indicate the oil changes. $\langle D \rangle$significantly changes over the runtime.

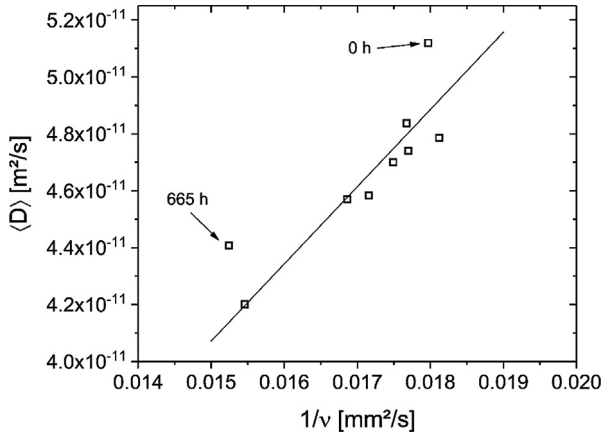

Fig. 6. Mean diffusion coefficient as a function of the inverse of the kinematic viscosity υ, at 313 K. □: the experimental data, the black line represents a fit of the Stokes-Einstein relation to the data (Eq. (11)). The two experimental quantities correlate nicely except for oils at engine runtimes of 0 h and 665 h.

the Stokes Einstein relation (Eq. (11)) as a very simplified approach under consideration of the density of the oil δ_{oil} 845kg/m^3 and using the radius R as a fit parameter, a linear correlation was found (Fig. 6).

The experimental data can be described by the Stokes Einstein relation, except for two points, which represent the data points for the fresh (t_{Engine} 0h) and the most degraded oils (t_{Engine} 665h). This means, that at a certain mileage the macroscopic viscosity does not correlate with the microscopic diffusion coefficient. The same is valid for the initial oil.

4.3. Impact of measurement temperature

Not only the magnetic field but also the measurement temper ature T has a significant influence on relaxation and diffusion. R_1 and its dispersion decrease with T (Fig. 7a).

Regarding the sensitivity towards oil aging, no differences depending on T were observed at 30 kHz (Fig. 7b). Transverse relaxation however does not show large differences as a function of T. With increasing T, $\langle R_2 \rangle$ decreases as well (Fig. 8a). The biggest relative differences between the aged oils and the fresh one occur at high temperatures (Fig. 8b), leading to the conclusion that the highest sensitivity regarding oil aging measuring $\langle R_2 \rangle$ is found at high temperatures for the investigated engine oils.

$\langle D \rangle$ increases with temperature for all investigated oil samples (Fig. 9a). Normalizing the values of aged oils to that of the fresh one, similar to R_1 no differences concerning T can be found regard ing the sensitivity of the measurement to aging effects (Fig. 9b). Depending on the measured NMR parameter, the measurement temperature plays a significant role only for transverse relaxation. The sensitivity of diffusion and longitudinal relaxation towards oil aging seems to be almost independent of T for the investigated oils. As R_2 is mainly sensitive to molecular fluctuations in the kHz range whereas R_1 is in the range of the much larger Larmor frequency, this finding leads us to the conclusion that the interesting fluctua tions to detect chemical changes during oil aging are in the lower frequency range. This finding is confirmed by the FFC results.

4.4. Single sided NMR

Both, NMR relaxation and diffusion are sensitive to aging pro cesses in engine oils. In QC, high throughput, ease of measurement and interpretation are essential. The question arises therefore whether NMR measurements can be designed such that R_1 or R_2 and D are recorded within one experiment. The parameters with their different sensitivity towards aging could then be explored at the same time. This possibility would lead to shorter measure ment times and an easier interpretation. One major challenge is to find the optimum measurement parameters as relaxation and diffusion phenomena are influenced by different environmental factors and therefore show different sensitivities regarding aging effects.

In order to measure diffusion and transverse relaxation at the same time, measurements with a single sided NMR device were performed. The CPMG pulse sequence was used under variation of the echo time τ_E. The data was analyzed using the Γ distribution model. With increasing echo time τ_E, $\langle R_{2eff} \rangle$ increases (Fig. 10a) while at first glance no clear trend is visible for the inves tigated engine oils. With regard to QC, the echo time giving the maximum differentiation between the oils has to be found.

Diffusion and transverse relaxation show opposite behavior with increasing oil runtime t_{Oil} (Fig. 3, Fig. 5b): the mean transverse relaxation rate increases and the diffusion coefficient decreases for the investigated oils. Taking into account, that both quantities affect the measurements using the single sided NMR device, no clear trend regarding the overall sensitivity was expected. To mea sure only transverse relaxation of liquids by a single sided NMR device, the echo time has to be chosen as short as possible to min imize diffusion effects. Weighing of the two contributions to the

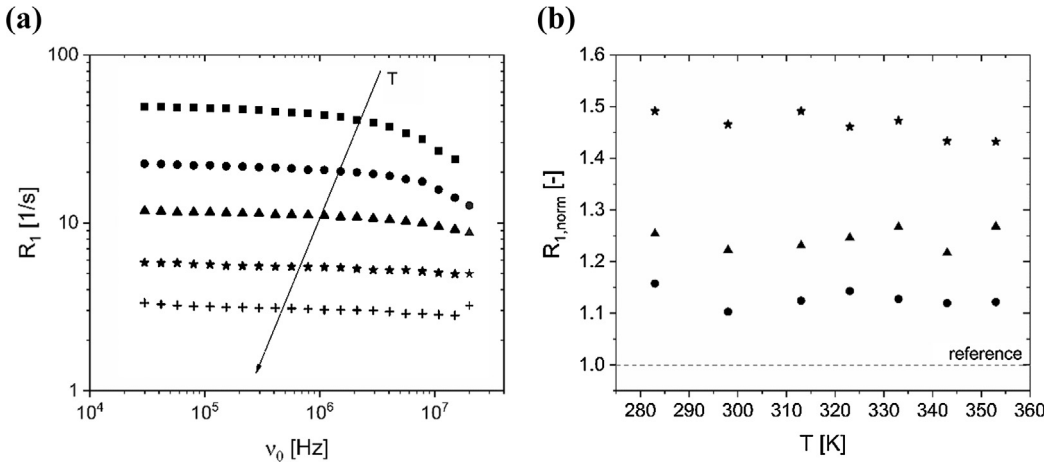

Fig. 7. (a) R_1 dispersion of the fresh oil (0 h) as a function of measurement temperature T. (T: 283 K (■), 298 K (●), 313 K (▲), 333 K (★) and 353 K (+)). With increasing T both, the absolute values and the dispersion decrease. The gray symbols at 20 MHz were measured using the Bruker "the minispec" mq20. (b) Relative longitudinal relaxation rate $R_{1,norm}$ of oils in the first oil change interval (reference line 0 h, ● 223 h, ▲ 429 h, ★ 665 h) as a function of the measurement temperature at 30 kHz. All oils are normalized to the value of the fresh oil (0 h) represented as a reference line. Independent of T the differences between the oils are constant.

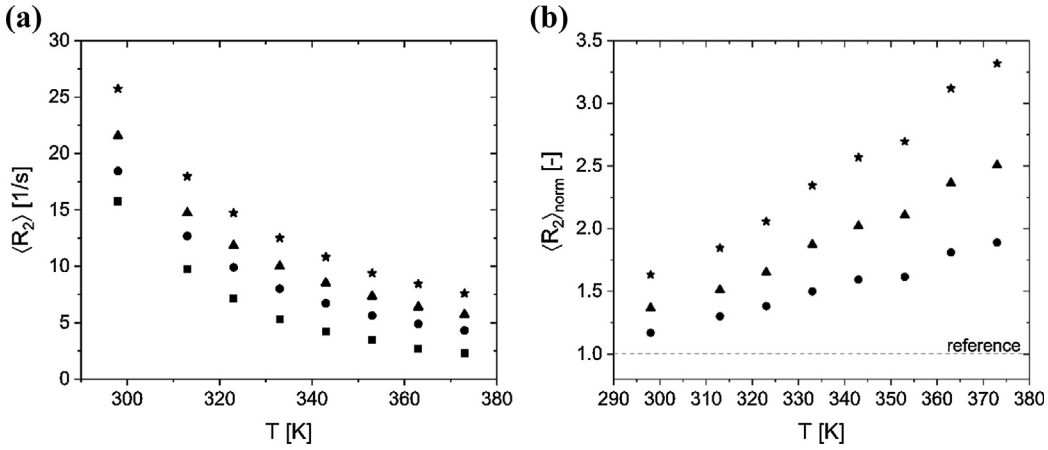

Fig. 8. (a) Mean transverse relaxation as a function of the measurement temperature T for different t_{Oil} (■ 0 h, ● 223 h, ▲ 429 h, ★ 665 h). $\langle R_2 \rangle$ decreases with T. (b) Relative mean transverse relaxation rate $\langle R_2 \rangle_{norm}$ of the first oil change interval (reference line 0 h, ● 223 h, ▲ 429 h, ★ 665 h) as a function of T. All oils are normalized to the fresh oil (0 h) represented as a reference line. The biggest differences between the oils occur at high temperatures.

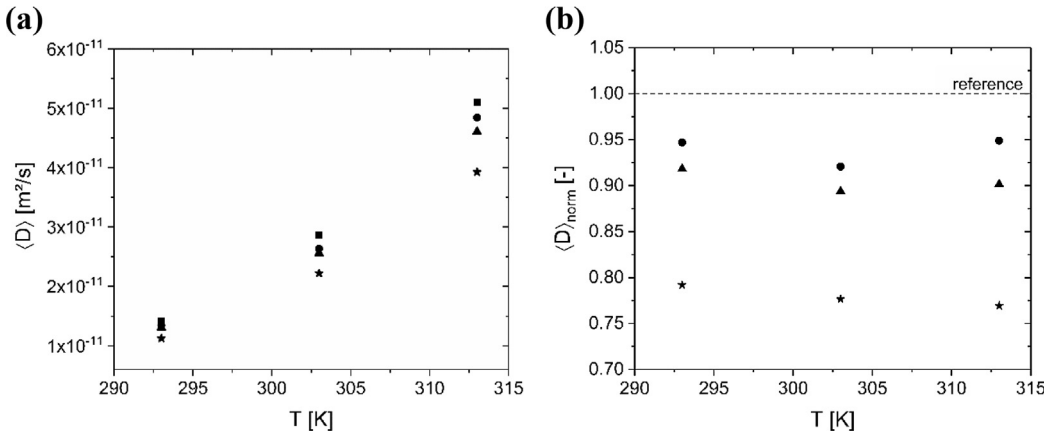

Fig. 9. (a) Mean diffusion coefficient as a function of the measurement temperature T for different t_{Oil} (■ 0 h, ● 223 h, ▲ 429 h, ★ 665 h). With increasing T, $\langle D \rangle$ increases. (b) Relative diffusion coefficients $\langle D \rangle_{norm}$ of the first oil change interval (reference line 0 h, ● 223 h, ▲ 429 h, ★ 665 h) as a function of T. All values were normalized to the fresh oil (0 h) represented as a reference line. The differences between the oils nearly stay constant.

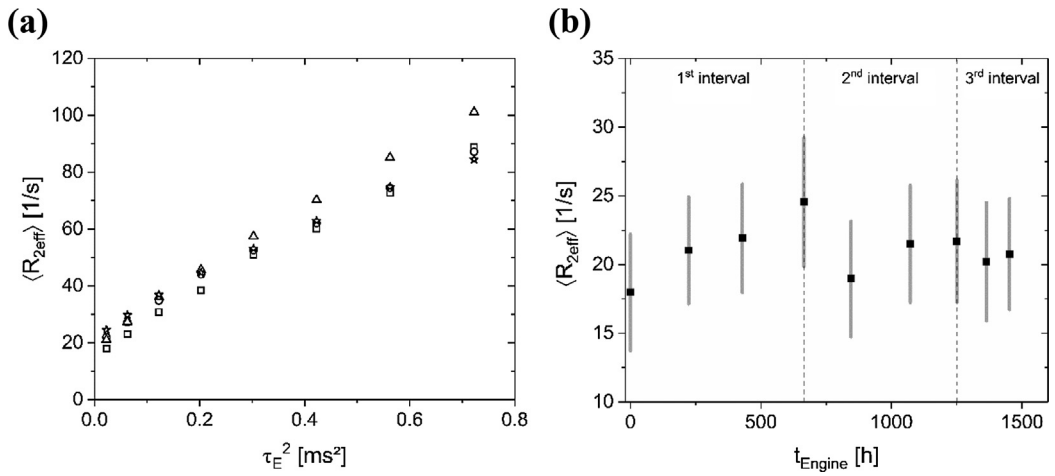

Fig. 10. (a) Effective relaxation rate as a function of squared echo time exemplarily for the oils of the first oil change interval: 0 h (□), 223 h (○), 429 h (△), 665 h (☆) at room temperature. (b) Effective relaxation rate $\langle R_{2eff} \rangle$ over the total engine runtime t_{Engine} at τ_E = 0.15 ms with increasing oil runtime, $\langle R_{2eff} \rangle$ also increases. Oil changes are nicely detectable while no sample preparation is needed.

transverse magnetization decay can be adjusted by the echo time. Thus, the same trend as in the R_2 measurements at 20 MHz (Fig. 3) results when plotting the mean effective relaxation rate $\langle R_{2eff} \rangle$ at τ_E = 0.l5 ms versus t_{Engine} (Fig. 10b). That is, the effective transverse relaxation rate increases with increasing oil runtime. After the oil changes, the relaxation rate starts to increase again while the most degraded oil sample is the oil after an engine runtime of 665 h. As a first trial, single sided NMR devices show a nice accordance with the measured transverse relaxation data using the Bruker "the minispec" mq20 and can further be explored towards QC of aged oils also at elevated temperatures, where the sensitivity towards aging is even more pronounced.

5. Conclusion

Engine oils at different degradation levels were investigated by diffusometry and time domain (TD) NMR relaxometry in order to characterize them exploiting molecular dynamics and to investi gate the possibilities of TD NMR in quality control (QC) of oils.

Largest sensitivities of R_1 to oil aging were measured at low magnetic fields independent of measurement temperature, indi cating that low frequency fluctuations are most sensitive to aging induced changes in engine oils.

Diffusion measurements showed nice correlation with the com monly measured kinematic viscosity. This indicates that the aver age molecular mass does not change with aging in this case of engine oils.

In relaxation and diffusion measurements, it was possible to detect aging. In contrast to longitudinal relaxation and diffusion, sensitivity towards oil aging increased with measurement temper ature in case of transverse relaxation. Considering the particulate contamination and viscosity in the description of the NMR transverse and longitudinal relaxation rate, the contribution of homonuclear dipolar relaxation characteristic for molecular mobility as well as of paramagnetic relaxation enhancement (PRE) could be estimated. NMR relaxometry therefore gives a bunch of information about the oil state as well as about (super) paramagnetic contaminants and aging processes in the engine oil. The use of single sided NMR is promising to obtain information about diffusion and relaxation simultaneously. In summary, TD NMR techniques were shown to be a powerful tool to analyze the degradation of oils also in the sense of QC.

Author contributions

The manuscript was written through contributions of all authors. All authors have given approval to the final version of the manuscript.

Acknowledgment

The authors thank all coworkers for the support in the NMR lab oratory at KIT and Universidad Nacional de Córdoba CONICET. EF acknowledges the Karlsruhe House of Young Scientists (KHYS) for the financial support for the research grant in Córdoba. DFG and AiF/ZIM are gratefully acknowledged for providing financial sup port for the instrumental facility center Pro^{2}NMR and to the project.

References

[1] L.R. Rudnick, Lubricant Additives: Chemistry and Applications, 2nd ed., CRC Press, Boca Raton, 2009.
[2] W.J. Bartz, Tribology, lubricants and lubrication engineering, Wear 49 (1978) 1–18.
[3] W. Dresel, Lubricants and Lubrication, John Wiley & Sons, 2007.
[4] E. Förster, J. Becker, F. Dalitz, B. Görling, B. Luy, H. Nirschl, G. Guthausen, NMR investigations on the aging of motor oils, Energy Fuel 29 (2015) 7204–7212.
[5] E. Förster, H. Nirschl, G. Guthausen, NMR diffusion and relaxation for monitoring of degradation in motor oils, Appl. Magn. Reson. 48 (2017) 51–65.
[6] A. Kupareva, P. Mäki-Arvela, H. Grénman, K. Eränen, R. Sjöholm, M. Reunanen, D.Y. Murzin, Chemical characterization of lube oils, Energy Fuels 27 (2013) 27–34.
[7] F. Owrang, H. Mattsson, J. Olsson, J. Pedersen, Investigation of oxidation of a mineral and a synthetic engine oil, Thermochim. Acta 413 (2004) 241–248.
[8] J.C.O. Santos, I.M.G.d. Santos, A.G. Souza, E.V. Sobrinho, V.J. Fernandes, A.J.N. Silva, Thermoanalytical and rheological characterization of automotive mineral lubricants after thermal degradation, Fuel 83 (2004) 2393–2399.
[9] L.L. Barbosa, F.V.C. Kock, V.M.D.L. Almeida, S.M.C. Menezes, E.V.R. Castro, Low-field nuclear magnetic resonance for petroleum distillate characterization, Fuel Process. Technol. 138 (2015) 202–209.
[10] L.L. Barbosa, F.V.C. Kock, R.C. Silva, J.C.C. Freitas, V. Lacerda, E.V.R. Castro, Application of low-field NMR for the determination of physical properties of petroleum fractions, Energy Fuel 27 (2013) 673–679.
[11] L.L. Barbosa, C.M.S. Sad, V.G. Morgan, P.R. Figueiras, E.R.V. Castro, Application of low field NMR as an alternative technique to quantification of total acid number and sulphur content in petroleum from Brazilian reservoirs, Fuel 176 (2016) 146–152.
[12] A. Guthausen, G. Guthausen, A. Kamlowski, H. Todt, W. Burk, D. Schmalbein, Measurement of fat content of food with single-sided NMR, J. Am. Oil Chem. Soc. 81 (2004) 727–731.

[13] H. Todt, W. Burk, G. Guthausen, A. Guthausen, A. Kamlowski, D. Schmalbein, Quality control with time-domain NMR, Eur. J. Lipid Sci. Technol. 103 (2001) 835–840.
[14] H. Todt, G. Guthausen, W. Burk, D. Schmalbein, A. Kamlowski, Water/moisture and fat analysis by time-domain NMR, Food Chem. 96 (2006) 436–440.
[15] I.U.o.P.a.A. Chemistry, Solid content determination in fats by NMR – Low resolution nuclear magnetic resonance, 1987.
[16] A.O.C. Society, Solid fat content (SFC) by low resolution magnetic resonance, AOCS, 1993.
[17] A.O.C. Society, Solid Fat Content (SFC) by Low-Resolution Nuclear Magnetic Resonance—The Direct Method, American Oil Chemists Society, 1997.
[18] Y. Gossuin, P. Gillis, A. Hocq, Q.L. Vuong, A. Roch, Magnetic resonance relaxation properties of superparamagnetic particles, Wiley Interdiscip Rev.-Nanomed. Nanobiotechnol. 1 (2009) 299–310.
[19] Q.L. Vuong, Y. Gossuin, P. Gillis, S. Delangre, New simulation approach using classical formalism to water nuclear magnetic relaxation dispersions in presence of superparamagnetic particles used as MRI contrast agents, J. Chem. Phys. 137 (2012).
[20] Q.L. Vuong, S. Van Doorslaer, J.L. Bridot, C. Argante, G. Alejandro, R. Hermann, S. Disch, C. Mattea, S. Stapf, Y. Gossuin, Paramagnetic nanoparticles as potential MRI contrast agents: characterization, NMR relaxation, simulations and theory, Magn. Reson. Mater. Phys. 25 (2012) 467–478.
[21] I. Bertini, C. Luchinat, G. Parigi, Solution NMR of Paramagnetic Molecules: Applications to Metallobiomolecules and Models, 1. ed., Elsevier Science B.V, Amsterdam, 2001.
[22] M. Röding, D. Bernin, J. Jonasson, A. Sarkka, D. Topgaard, M. Rudemo, M. Nyden, The gamma distribution model for pulsed-field gradient NMR studies of molecular-weight distributions of polymers, J. Magn. Reson. 222 (2012) 105–111.
[23] R. Kimmich, E. Anoardo, Field-cycling NMR relaxometry, Prog. Nucl. Magn. Reson. Spectr. 44 (2004) 257–320.
[24] F. Noack, NMR field-cycling spectroscopy: principles and a] lications, Prog. Nucl. Magn. Reson. Spectr. 18 (1986) 171–276.
[25] E. Anoardo, G. Galli, G. Ferrante, Fast-field-cycling NMR: applications and instrumentation, Appl. Magn. Reson. 20 (2001) 365–404.
[26] M. Ballari, F. Bonetto, E. Anoardo, NMR relaxometry analysis of lubricant oils degradation, J. Phys. D Appl. Phys. 38 (2005) 3746.
[27] N. Bloembergen, E.M. Purcell, R.V. Pound, Relaxation effects in nuclear magnetic resonance absorption, Phys. Rev. 73 (1948) 679–712.
[28] H.C. Torrey, Bloch equations with diffusion terms, Phys. Rev. 104 (1956) 563–565.
[29] A. Abragam, The Principles of Nuclear Magnetism, Oxford University Press, 1961.
[30] S. Meiboom, D. Gill, Modified spin-echo method for measuring nuclear relaxation times, Rev. Sci. Instr. 29 (1958) 688–691.
[31] P.T. Callaghan, Principles of Nuclear Magnetic Resonance Microscopy, Oxford University Press, New York, 1991.
[32] B. Blümich, P. Blümler, G. Eidmann, A. Guthausen, R. Haken, U. Schmitz, K. Saito, G. Zimmer, The NMR-MOUSE: construction, excitation, and applications, Magn. Reson. Imaging 16 (1998) 479–484.
[33] A. Guthausen, Die NMR-MOUSE: Methoden und Anwendungen zur Charakterisierung von Polymeren, Makromol. Chem., RWTH Aachen, Aachen, 1998.
[34] G. Guthausen, A. Guthausen, F. Balibanu, R. Eymael, K. Hailu, U. Schmitz, B. Blümich, Soft-matter analysis by the NMR-MOUSE, Macromol. Mater. Eng. 276 (2000) 25–37.
[35] R. Eymael, Messung von molekularer Selbstdiffusion mit kernmagnetischer Resonanz in Aufsatztechnik, Makromol. Chem., RWTH Aachen, Aachen, 1997.
[36] R. Kashaev, Viscosity correlations with nuclear (Proton) magnetic resonance relaxation in oil disperse systems, Appl. Magn. Reson. 49 (2018) 309–325.
[37] G.G. Stokes, On the effect of the internal friction of fluids on the motion of Pendulums, Cambridge Philos. Soc. Trans. 9 (1851) 8–106.